frontiers in Pharmacology

ORIGINAL RESEARCH
published: 03 August 2021
doi: 10.3389/fphar.2021.680618

High-Throughput Drug Screening System Based on Human Induced Pluripotent Stem Cell-Derived Atrial Myocytes ~ A Novel Platform to Detect Cardiac Toxicity for Atrial Arrhythmias

Yayoi Honda[1,2], *Jun Li*[3,4], *Aya Hino*[4], *Shinji Tsujimoto*[1] *and Jong-Kook Lee*[4]*

[1]Sumitomo-Dainippon Pharma CO., Ltd., Osaka, Japan, [2]Bioanalysis Group, Osaka Laboratory, Technical Solution Headquarters, Sumika Chemical Analysis Service, Ltd., Osaka, Japan, [3]Department of Cardiovascular Medicine, Osaka University Graduate School of Medicine, Suita, Japan, [4]Department of Cardiovascular Regenerative Medicine, Osaka University Graduate School of Medicine, Suita, Japan

OPEN ACCESS

Edited by:
Tamer M. A. Mohamed,
University of Louisville, United States

Reviewed by:
InKyeom Kim,
Kyungpook National University, South Korea
Matthew A. Nystoriak,
University of Louisville, United States

***Correspondence:**
Jong-Kook Lee
jlee@cardiology.med.osaka-u.ac.jp

Specialty section:
This article was submitted to Cardiovascular and Smooth Muscle Pharmacology, a section of the journal Frontiers in Pharmacology

Received: *15 March 2021*
Accepted: *13 July 2021*
Published: *03 August 2021*

Citation:
Honda Y, Li J, Hino A, Tsujimoto S and Lee J-K (2021) High-Throughput Drug Screening System Based on Human Induced Pluripotent Stem Cell-Derived Atrial Myocytes ~ A Novel Platform to Detect Cardiac Toxicity for Atrial Arrhythmias. Front. Pharmacol. 12:680618. doi: 10.3389/fphar.2021.680618

Evaluation of proarrhythmic properties is critical for drug discovery. In particular, QT prolongation in electrocardiograms has been utilized as a surrogate marker in many evaluation systems to assess the risk of torsade de pointes and lethal ventricular arrhythmia. Recently, new evaluation systems based on human iPS cell-derived cardiomyocytes have been established. On the other hand, in clinical situations, it has been reported that the incidence of atrial arrhythmias such as atrial fibrillation has been increasing every year, with the prediction of a persistent increase in the near future. As to the increased incidence of atrial arrhythmias, in addition to the increased population of geriatric patients, a wide variety of drug treatments may be related, as an experimental method to detect drug-induced atrial arrhythmia has not been established so far. In the present study, we characterized the atrial-like cardiomyocytes derived from human induced pluripotent stem cells and examined their potential for the evaluation of drug-induced atrial arrhythmia. Atrial-like cardiomyocytes were induced by adding retinoic acid (RA) during the process of myocardial differentiation, and their characteristics were compared to those of RA-free cardiomyocytes. Using gene expression and membrane potential analysis, it was confirmed that the cells with or without RA treatment have atrial or ventricular like cardiomyocytes, respectively. Using the ultra-rapid activating delayed rectifier potassium current (I_{Kur}) channel inhibitor, which is specific to atrial cardiomyocytes, Pulse width duration (PWD) 30cF prolongation was confirmed only in atrial-like cardiomyocytes. In addition, ventricular like cardiomyocytes exhibited an early after depolarization by treatment with rapidly activating delayed rectifier potassium current (I_{Kr}) channel inhibitor, which induces ventricular arrhythmia in clinical situations. Here, we have established a high-throughput drug evaluation system using human iPS cell-derived atrial-like cardiomyocytes. Based on the obtained data, the system might be a valuable platform to detect potential risks for drug-induced atrial arrhythmias.

Keywords: human iPS cell-derived atrial-like cardiomyocytes, nodal-like cardiomyoyctes, atrial arrhythmias, sick sinus syndrome, drug screening

INTRODUCTION

It has been reported that 22% of candidate compounds dropped out at the developmental stage of new drugs and 45% of pharmaceutical products were withdrawn from the market (Watkins, 2011). Therefore, in research and development, it is critical to detect cardiotoxicity during the selection of appropriate compounds for new drugs. In particular, drug-induced torsade de pointes (TdP) has been the most serious concern as it leads to ventricular fibrillation or sudden death.

In western countries, cases of TdP-related death were frequently reported in the late 80s through the early 90s. Several pharmaceutical products were withdrawn from the market because of their risk of inducing TdP in the early 90s (Thomsen et al., 2006; Stockbridge et al., 2013). The International Council for Harmonisation of Technical Requirements for Pharmaceuticals for Human Use (ICH) guidelines for cardiotoxicity evaluation (non-clinical: S7B, clinical: E14), therefore, were enforced to handle these situations, and there have been few examples of product withdrawal due to TdP after the launch of ICH guidelines (Stockbridge et al., 2013). In recent years, human induced pluripotent stem cell-derived cardiomyocytes (hiPSC-CMs) in which ventricular cardiomyocytes are dominant have been commercially available, and multi-facility validation studies using these cells to improve the predictability of drug-induced arrhythmia evaluation have been in progress (Nozaki et al., 2017; Ando et al., 2017).

Cases of not only ventricular but also atrial arrhythmia are also known in clinical situations. Atrial arrhythmia indicates some phenotypes including tachyarrhythmia such as atrial flutter or fibrillation, or bradyarrhythmia such as sick sinus syndrome or atrioventricular block. In tachyarrhythmia, atrial fibrillation occasionally induces cardiac arrest caused by a deterioration of contraction, atrial thrombus formation, and related infarction in organs/tissues. Bradyarrhythmia also causes transient cardiac arrest accompanied by loss of consciousness or cardiac arrest. Although the fatality rate caused by atrial arrhythmia itself is not very high, some lethal diseases originating from atrial arrhythmia are known. The incidence of atrial arrhythmia has increased annually in recent decades (Jensen et al., 2012; Chugh et al., 2014; Schnabel et al., 2015; Lane et al., 2017) and it is predicted that the number of patients will be growing (Jensen et al., 2014; Lane et al., 2017). Aging can be thought of as one of its risk factors, and an aging society might be related to an increase in the number of atrial arrhythmias. Several medicines, such as calcium antagonists, beta-adrenergic blockers, or antipsychotic agents, induce bradyarrhythmia (Edoute et al., 2000; Berry and Hasin, 1978; Johnson et al., 1997; Bordier et al., 2003). Not only aging but also drug treatment may be a trigger for tachyarrhythmia. As the evaluation tools for atria arrhythmia have not been established thus far, we could not confirm the existence of drug-induced atrial arrhythmia itself.

As ventricular cardiomyocytes are dominant in commercially available hiPSC-CMs, atrial arrhythmia might not be detected using these cells. Retinoic acid (RA) is essential in the regulation of cardiac development (Moss et al., 1998). Inhibition of RA synthesis induced the lack of atrial chamber in mouse embryo heart (Xavier-Neto et al., 1999). Hidaka et al.(2003) established a differentiation protocol from mouse embryonic stem (ES) cells to cardiomyocytes, and confirmed that retinoic acid induced atrial cardiomyocytes from ES cells. In recent years, retinoic acid has also been used for inducing atrial cardiomyocyte from human ES/iPS cells Zhang et al. (2011), Gassanov et al. (2008), Lee et al. (2017), and these differentiation methods have been proposed for the application of pathophysiological models of atrial arrhythmia or drug screening for atrial arrhythmia (Devalla et al., 2015; Argenziano et al., 2018; Lemme et al., 2018). In the present study, we obtained a hiPS-derived atrial-like phenotype by supplemented RA during the cardiac mesoderm induction. Accordingly, we tried to examine the acute response to drug administration in the hiPS-CMs with (atrial-like subtype) or without (ventricular-like subtype) treatment of RA.

RESULTS

Cardiac Differentiation Induction From hiPSCs

Undifferentiated hiPSCs were maintained in AK02 medium for 2–3 days until 80% confluency was obtained. Cardiac differentiation was then induced according to the manufacturer's protocol, as shown in **Figure 1A**. To obtain highly purified cardiomyocytes, metabolic selection was performed during post-differentiation, from day 15–26. Cardiomyocyte proportion was quantified by immunostaining with cardiac troponin-T (cTnT). **Figure 1B** shows that the proportion of cTnT-positive cells was over 90% with or without RA treatment (CT 93.9 ± 2.51% vs. AM 96.8 ± 1.81%). The results suggest that RA application did not influence cardiomyocyte differentiation efficiency.

Characteristics of hiPS-Derived Cardiomyocytes With RA Treatment

To further evaluate the gene expression of cardiac subtypes in the control hiPS-CMs (CT) and the RA-treated hiPS-CMs (AM), the cells were co-stained with myosin light chain 2a (MLC-2a: atrial isoform) and myosin light chain 2v (MLC-2v: ventricular isoform) (**Supplementary Figure 1**). An immunofluorescence study showed that the ratio of MLC-2a positive cells and MLC-2v positive cells are comparable in CT (MLC-2a 56.0 ± 2.1% vs. MLC-2v 57.0 ± 2.11%), and the percentage of double-positive cells (MLC-2a$^+$/MLC-2v$^+$) was approximately 40%. In AM (MLC-2a 83.4 ± 0.63%), most cTnT-positive cells were co-positive for MLC-2a, however, very few cTnT-positive cells were found co-positive for MLC-2v (MLC-2v 14.0 ± 2.82%) (**Figures 1B, C**).

To analyze the differences in the functional and electrophysiological properties of atrial and ventricular cardiomyocytes, we assessed multiple parameters of the action potential in CT and AM using a voltage-sensitive dye.

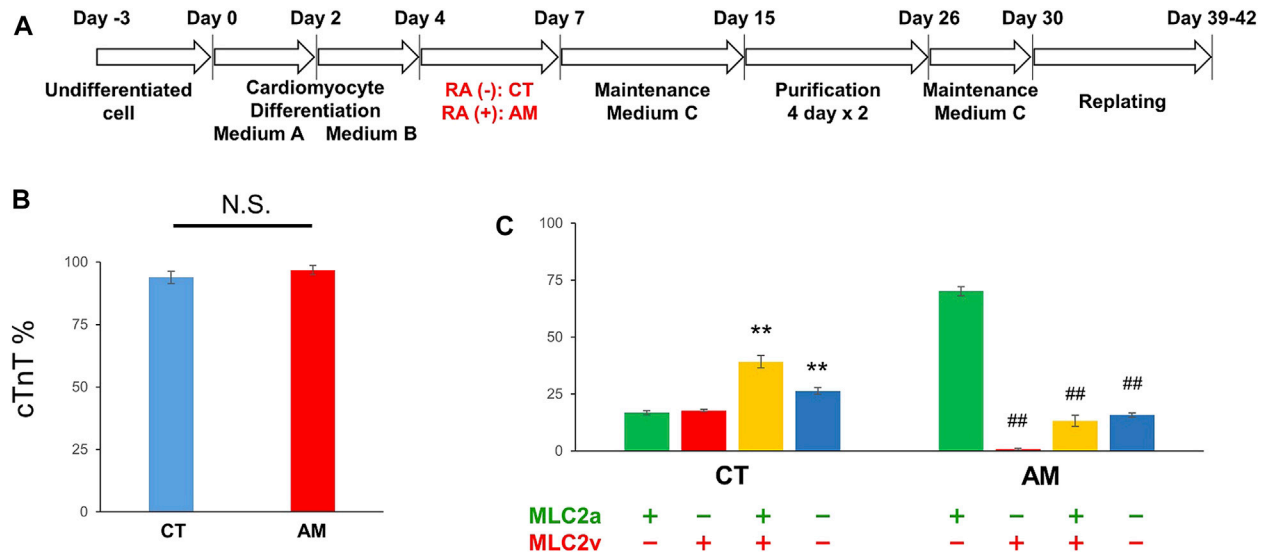

FIGURE 1 | Cardiac differentiation from hiPSCs **(A)** Schematic of the protocol for the differentiation of cardiomyocytes from hiPS cells with (RA (+)) or without RA (RA (–)) treatment **(B)** The ratio of cardiomyocytes quantified by immunostaining with cardiac troponin-T (cTnT). The proportion of cTnT positive cells was 93.91 ± 2.51% in CT (control hiPS-CMs), or 96.79 ± 1.81% in AM (RA-treated hiPS-CMs), respectively (P = N.S.). Error bars represent SD of the mean from the values of independent experiments. *n* = 3. N.S., not significant **(C)** Immunofluorescence analysis of the percentage of MLC2a (atrial isoform) and MLC2v (ventricular isoform) positive expression in the CT and AM. Error bars represent SD of the mean from the values of independent experiments. $^{**}p < 0.01$ for comparison with MLC 2a+/MLC 2v-cardiomyocyte in CT, $\#\#p < 0.01$ for comparison with MLC 2a+/MLC 2v-cardiomyocyte in AM, *n* = 3.

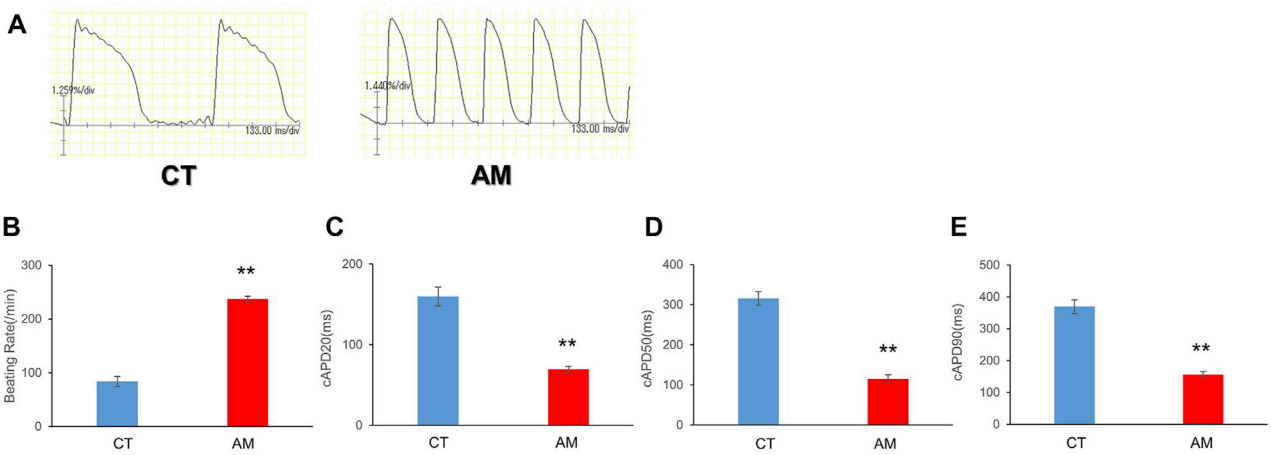

FIGURE 2 | Optical action potential (OAP) of CT (control hiPS-CMs) or AM (RA treatment hiPS-CMs). Representative waveforms for AP of CT or AM. The comparison of AP parameters: beating rate, cAPD20, cAPD50, and cAPD90, between CT and AM. Error bars represent SD of the mean from the values of independent experiments. $^{**}p < 0.01$, *n* = 3.

To examine the electrophysiological properties, we conducted optical mapping of action potentials based on spontaneous beating cardiomyocytes. The AP of AMs displayed a spike-like shape with a steep upslope and downslope, as well as a high frequency, which was more than twice that of CT (**Figures 2A, B**. CT 83.7 ± 9.50/min vs. AM 237 ± 5.20/min). In addition, the action potential duration in AM was significantly shorter than that in CT (**Figures 2C–E**. CT vs. AM: $cAPD_{20}$: 159.8 ± 11.7 vs. 69.8 ± 3.66 ms; $cAPD_{50}$ 315.5 ± 16.93 vs. 114.9 ± 10.7 ms; $cAPD_{90}$ 369.7 ± 21.7 vs. 156.1 ± 9.19 ms).

The above data suggested more atrial-like properties in ATRA-treated AM compared with that of control CT.

High-Throughput Drug Testing Using hiPS-Derived Atrial Myocytes

Using a high-throughput screening system (FDSS/μCell), we assessed the drug toxicity of several experimental drugs on hiPS-derived atrial myocytes as well as control hiPS-derived cardiomyocytes. Membrane potential was used as one of the parameters during the assessment.

After purification, hiPS-derived cardiomyocytes were plated in 96-well plates for downstream drug response assessment using FluoVolt™ Membrane Potential Kit. The results of the analysis of membrane potentials are summarized in **Table 1**. For the proper evaluate the variance of electrophysiological response in CT and AM after drug administration, we have recorded the baseline data of CT and AM respectively (**Supplementary Table 1**). The comparison of variance in the response of drug administration in CT and AM was represented by the percentage of changes based on their baseline values respectively.

hiPS-derived cardiomyocytes without RA (CT) or with RA (AM) were applied with an incremental concentration of I_{Kr} blockers: E-4031, donepezil, and propranolol. The application of E-4031 (0.0003–0.1 μM), donepezil (0.03–10 μM), and propranolol (0.1–100 μM) showed a dose-dependent decrease in beating rate, rising slope, and falling slope of membrane potential in both the CT and the AM (**Figure 3**, **Supplementary Figure 2**). PWD (Pulse width duration) 80cF and PWD30-80 were prolonged as the drug concentration increased. Although under the 0.1 μM E-4031 conditions, both CT and AM showed an increase in membrane potential duration, EAD was elicited in CT (**Figure 3**).

As presented in **Table 2**, E-4031 treatment increased the incidence of EAD in a dose-dependent manner. When treated with 10 μM donepezil on CT, EAD was observed in 2 of 6 cases, while cessation of beating was observed in the remaining 4 cases. However, all of the wells appeared to stop beating in AM under the same dose of donepezil. For the application of propranolol, the CT showed irregular beating or the EAD appeared once the concentration was above 10 μM. Cessation of beating was observed in all cases at a 100 μM dose of propranolol. In the AM, 1 out of 9 samples showed irregular beating at a 10 μM dose of propranolol, and all wells ceased beating at concentrations higher than 30 μM.

With the application of the I_{Ks} channel blocker Chromanol 293B in the range of 0.3–100 μM, CT either AM exhibited a dose-dependent decrease in the rising slope of membrane potential, while an increase in the membrane potential duration was observed (data not shown). When a dose under 100 μM of Chromanol 293B was administered, cessation of beating appeared in 2 of 9 samples in CT and 3 of 12 samples in AM.

To evaluate the response of CT or AM to the I_{Kur} channel blockers, 4-Aminopiridine (4-AP) (0.3–100 μM), DPO-1 (0.01–3 μM), and S9947 (0.03–10 μM) were used within various dose ranges, respectively (**Figure 4**). In AM, the application of 4-AP and DPO-1 exhibited dose-dependent increases in PWD30cF and PWD50cF. S9947 treatment of AM led to a dose-dependent increase in membrane potential duration, and was the highest in PWD30cF. All of the AM samples were arrested after application of 10 μM of S9947, although the half cases were arrested on CT accompanied by a decrease in the amplitude of membrane potential.

Carbachol, which can activate I_{KAch} current, led to a decrease in the beating rate and rising slope of membrane potential in AM; however, no significant difference was observed in the response to CT (**Table 1**). No irregular beating or EAD was elicited on CT either in AM.

As widely used drugs for cardiovascular diseases, the calcium ion channel blocker verapamil and diltiazem, as well as the selective calcium channel activator Bay K8644, were also tested at various concentrations (**Figure 5**, **Supplementary Figure 3**). For CT, verapamil and diltiazem showed dose-dependent increases in beating rate and falling slope of membrane potential. Accordingly, the membrane potential durations decreased, especially for PWD30cF and PWD50cF. However, in AM, except for the dose-dependent increase in the beating rate, no obvious changes were observed in other parameters of membrane potential. At 0.1 μM doses of verapamil and diltiazem, all the AM samples showed cessation of beating. In contrast, Bay K8644 showed a dose-dependent decrease in the falling slope of membrane potential and prolonged membrane potential duration in both CT and AM samples. The CT either AM showed an acute response to Bay K8644, and PWD30 prolonged significantly (**Table 1**).

Carbamazepine treatment in CT led to a decrease in the beating rate and the rising slope of membrane potential, as well as an increase in falling slope and shortened membrane potential duration in a dose-dependent manner (**Figure 6**, **Supplementary Figure 4**). Irregular beating and cessation of beating were induced over application of concentrations above 30 μM. At 100 μM, 11 of 12 cases in CT showed arrest of beating (**Table 2**). In contrast, in AM, no obvious change was observed except a decrease in the rising slope of the membrane potential. However, cessation of beating was observed in half the cases and 5 of 6 cases at concentrations of 30 μM and 100 μM, respectively (**Table 2**).

The effect of phenytoin on CT was characterized by a dose-dependent decrease in the rising slope and an increase in the falling slope of membrane potential (**Figure 6**, **Supplementary Figure 4**). Cessation of beating was elicited when the concentration was higher than 30 μM (**Table 2**). In AM samples, there was also a dose-dependent decrease in the rising slope of membrane potential, though cessation of beating was elicited at the concentration higher than 10 μM. Furthermore, the incidence of cessation of beating increased in a dose-dependent manner (**Table 2**).

DISCUSSION

In the present study, we established a high-throughput drug testing system using human iPS cells derived atrial-like myocytes based on our previous reports (Nakanishi et al., 2019; Hidaka et al., 2003).

The protocol successfully yielded atrial-like myocytes with adequate quality and efficiency, similar to the previous report by (Argenziano et al., 2018).

TABLE 1 | Effects of test compounds in MP of CT or AM. The change scopes of MP parameters are represented by the width of % change.

Drug		Beat Rate	Rising Slope	Falling Slope	PWD30cF	PWD80cF
E-4031	CT	↓	↓↓	↓↓	↓	↑↑
I_{Kr} inhibition	AM	↓	↓	↓↓		↑
Chromanol 293B	CT		↓	↓	↑	↑
I_{Ks} inhibition	AM		↓		↑	
4-Aminopridine	CT				↑	
I_{Kur} inhibition	AM				↑	↑
DPO-1	CT					
I_{Kur} inhibition	AM				↑	
S9947	CT	↓↓	↓↓	↑	↓	↓
I_{Kur} inhibition	AM				↑↑	↑
Carbachol	CT					
I_{KAch} activation	AM	↓	↓			
Verapamil	CT	↑↑	↓	↑↑	↓↓	↓
Cav1.2 inhibition	AM	↑				
Diltiazem	CT	↑↑		↑↑	↓↓	↓
Cav1.2 inhibition	AM	↑			↓	
Bay K 8644 (3 min)	CT			↓	↑	↑
Cav1.2 activation	AM		↑	↓	↑	↑
Propranolol	CT	↓↓	↓↓	↓↓	↓	↑
Nav1.5, IKr inhibition	AM	↓↓	↓↓	↓		↑
Donepezil	CT	↓	↓	↓↓		↑
IKr inhibition	AM	↓↓	↓	↓↓	↑	↑
Carbamazepine	CT	↓	↓↓	↑	↓	↓
	AM		↓↓			
Phenytoin	CT		↓	↑		
	AM		↓			

Width of % change : ↑↓ 20~30%, ↑ ↓ 30~50%, ↑↑ ↓↓ 50%~

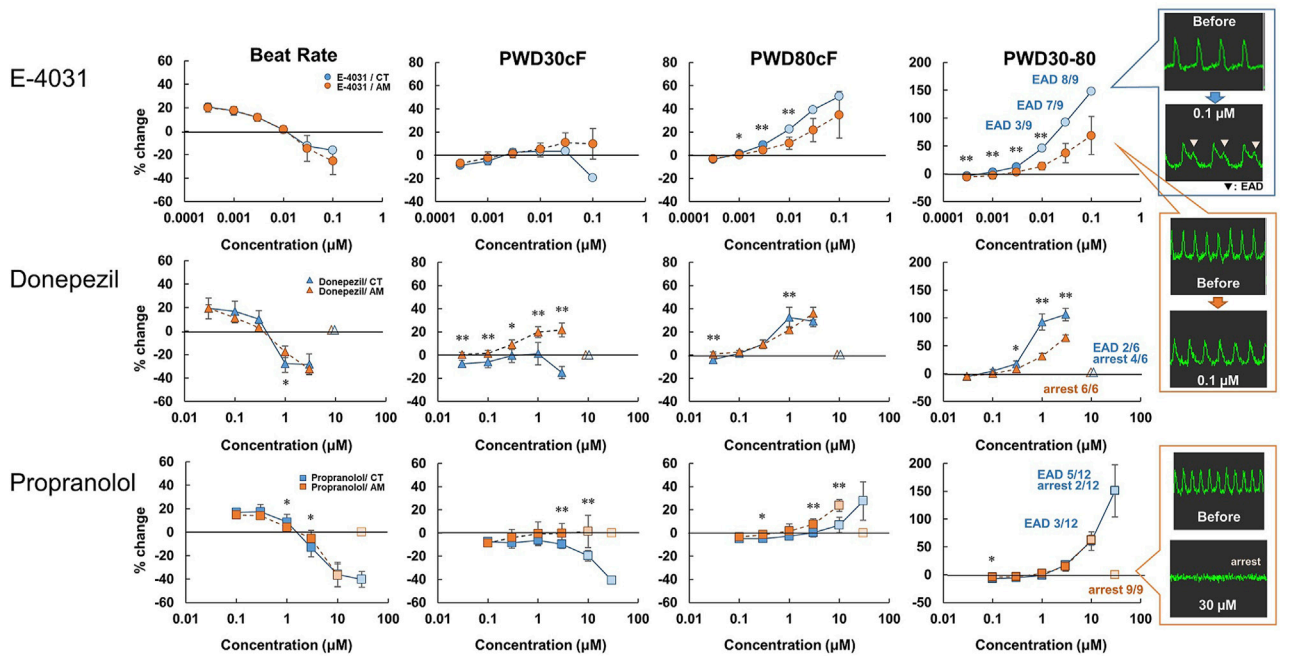

FIGURE 3 | Dose-response of I_{Kr} blockers in CT and AM. CT and AM were treated with various concentrations of E-4031, donepezil, and propranolol, and membrane potential (MP) was analyzed by FDSS/μCell imaging platform. *Y*-axis represents the percentage change from the value before test compound addition. Comparison of MP parameters: beat rate, PWD30cF, PWD80cF, PWD30-80 in CT and AM. Error bars represent SD of the mean from the values of independent experiments. n = 3–12. $^{*}p < 0.05$, $^{**}p < 0.01$ for comparison of drug treatment of CT vs. AM (right-most panel) representative waveforms for MP in CT or AM after application of 0.1 μM E-4031. Although both CT and AM showed an increase in membrane potential duration, EAD was elicited in CT. E-4031 data: reuse from the conference paper with permission (Honda, 2020).

In RA-treated myocytes, gene expression levels showed a decrease in ventricle-specific transcription factor IRX4 and an increase in atrium-specific NPPA. On the other hand, those of cardiac ion channels such as Ca^{2+} and K^{+} channels, which constitute action potentials, were expressed in both groups, while atrial specific channels such as KCNA5 and KCNJ3 were significantly increased in RA-treated myocytes. These results suggest that RA treatment induces atrial differentiation, similar

TABLE 2 | Effects of test compounds on arrhythmia-like waveforms in CT or AM. The blue frame indicates drug application concentration. Values indicate an incidence of arrhythmia-like waveforms; green column: irregular beat, yellow column: arrest, red column: EAD.

Drug		n	Concentration (μM)												
			0.0001	0.0003	0.001	0.003	0.01	0.03	0.1	0.3	1	3	10	30	100
E-4031	CT	6					50%	83%	83%						
I_{Kr} inhibition	AM	6													
Chromanol 293B	CT	9													22%
I_{Ks} inhibition	AM	12													25%
4-Aminopridine	CT	6													
I_{Kur} inhibition	AM	6													
DPO-1	CT	6													
I_{Kur} inhibition	AM	6													
S9947	CT	6											50%		
I_{Kur} inhibition	AM	6											100%		
Carbachol	CT	9													
I_{KAch} activation	AM	12													
Verapamil	CT	6													
Cav1.2 inhibition	AM	6							100%						
Diltiazem	CT	6													
Cav1.2 inhibition	AM	6									100%				
BayK8644	CT	6													
Cav1.2 activation	AM	6													
Propranolol	CT	3-12											17%	25% 8% 42% 17%	100%
Nav1.5, I_{Kr} inhibition	AM	3-9											11%	100%	100%
Donepezil	CT	6											33%	67%	
I_{Kr} inhibition	AM	6											100%		
Carbamazepine	CT	12												25% 8%	8% 92%
	AM	6												50%	83%
Phenytoin	CT	6												83%	100%
	AM	6											50%	67%	100%

Blue frame shows drug application concentration. Values indicate an incidence of arrhythmia-like waveforms; green column: irregular beat, yellow column: arrest, red column: EAD

to previous reports (Devalla et al., 2015; Argenziano et al., 2018; Lemme et al., 2018; Nakanishi et al., 2005).

The measurement of cardiac action potentials has been used in the research of disease modeling and drug discovery based on hiPS-derived cardiomyocytes, since APs directly recapitulate patients' pathophysiological conditions and reflect the efficacy and cardiotoxicity of pharmacological compounds as drug candidates. Although patch-clamp techniques have been widely used for single-cell-based precise electrophysiological testing, the technique is not suitable for high-throughput screening systems. Thus, in the present study, we employed optical recording using membrane potential dyes (FluoVolt™).

As shown in **Figure 2**, the optical action potentials of CT demonstrated the "plateau" phase, while the shorter action potentials of AM demonstrated a lack of "plateau." This property was recognized as the difference of the ratio APD_{30-40}/APD_{70-80} in CT (1.30 ± 0.18) and in AM (0.75 ± 0.11) (data not shown). Although the data in the present study was less than the data reported by Argenziano et al. (APD_{30-40}/APD_{70-80}: 0.97 ± 0.12 in CT and AM 0.48 ± 0.0), this may be ascribed to the difference in beating rates (Argenziano et al., 2018).

Based on these properties, hiPS-CTs and hiPS-AMs can be considered stable platforms for electrophysiological testing for drug discovery and development, although the cells may have an immature nature compared to native cardiomyocytes, as reported previously (Feric and Radisic, 2016).

I_{Kr} Blockers

We further verified the feasibility of detecting atrial-specific responses of various pharmacological compounds. In the present study, we examined the effect of E-4031 (an I_{Kr} blocker) on OAP parameters in CT and AM As a result, E-4031 caused dose-dependent increases in PWD80cF and PWD30-80, and a decrease in the rising slope and falling slope in both CT and AM (**Figure 3**, **supplementary Figure 2**). These results are comparable to the previous report by Knobloch stating that I_{Kr} blockers prolonged ventricular repolarization and the atrial refractory period (Knobloch et al., 2002). In addition, it is known that I_{Kr} blockers cause QT prolongation and induce ventricular arrhythmias. Thus, previous papers reported that I_{Kr} blockers showed characteristic proarrhythmic changes in action potentials in ventricular-rich-hiPS-CMs (Ma et al., 2011; Nozaki et al., 2017). In the present study, since EADs were observed in CT but not in AM (**Figure 3**; **Table 2**), induction of proarrhythmic propensity by I_{Kr} blockers in the hiPS-based platform was a ventricular specific phenomenon. Based on this observation, our platform clearly showed the difference between control (induction of arrhythmias) and atrial platform (inhibition of arrhythmias).

Donepezil (Anti-dementia Drug)

Donepezil is a choline esterase inhibitor used to treat Alzheimer's disease and dementia with Lewy bodies, and the drug shows I_{Kr} blocking action with various critical side effects including QT prolongation and lethal ventricular arrhythmias (Kho et al., 2021). Our present data showed that donepezil prolonged the membrane potential duration at a concentration consistent with previous reports 1.3–9.9 μM (Chae et al., 2015) (**Figure 3**). It has been also reported that the drug causes bradyarrhythmias (Rosenbloom et al., 2010; Kuwahata et al., 2021). In the present study, consistent with the

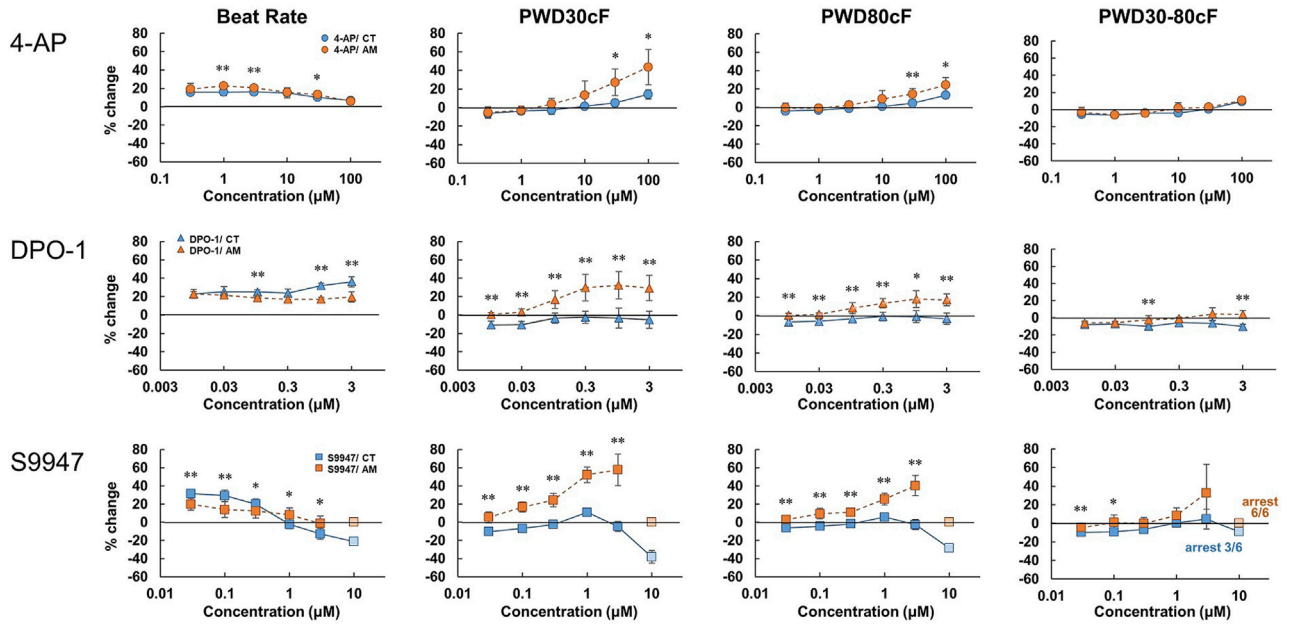

FIGURE 4 | Dose-response of I_{Kur} channel blockers in CT and AM. CT and AM were treated with various concentrations of 4-Aminopiridine (4-AP), DPO-1, and S9947, and MP was analyzed by FDSS/μCell imaging platform. *Y*-axis represents the percentage change from the value before test compound addition. Comparison of MP parameters: beat rate, PWD (Pulse width duration) 30cF, PWD80cF, PWD30-80cF in CT and AM. Error bars represent SD of the mean from the values of independent experiments. n = 6, $^{*}p < 0.05$, $^{**}p < 0.01$ for comparison of drug treatment of CT vs. AM. DPO-1 data: reuse from the conference paper with permission (Honda, 2020).

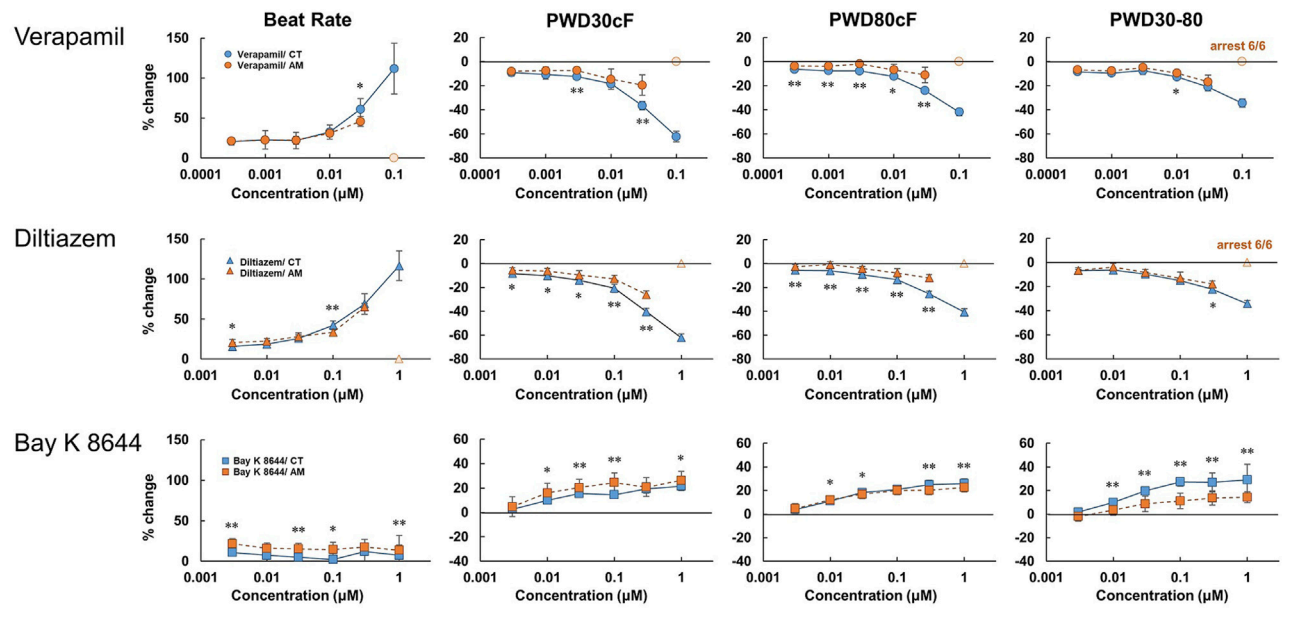

FIGURE 5 | Dose-response of calcium ion channel regulator in CT and AM. Comparison of MP parameters: beat rate, PWD30cF, PWD80cF, PWD30-80 in CT and AM after application of calcium ion channel blocker verapamil and diltiazem, as well as the selective calcium channel activator Bay K 8644. Error bars represent SD of the mean from the values of independent experiments. $n = 6$. $^{*}p < 0.05$, $^{**}p < 0.01$ for comparison of drug treatment of CT vs. AM. Bay K8644 data: reuse from the conference paper with permission (Honda, 2020).

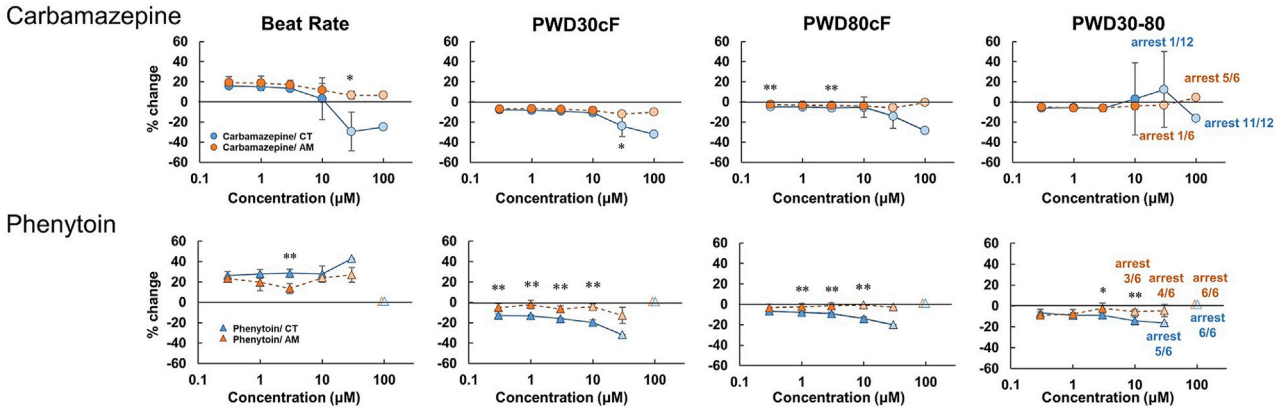

FIGURE 6 | Dose-response of sodium ion channel regulator in CT and AM. Comparison of MP parameters: beat rate, PWD30cF, PWD80cF, PWD30-80 in CT and AM after application of carbamazepine and phenytoin. Error bars represent SD of the mean from the values of independent experiments. n = 6–12. $^{*}p < 0.05$, $^{**}p < 0.01$ for comparison of drug treatment of CT vs. AM.

reports, the drug induced the cessation of spontaneous beating in AM and CT at the concentration higher than 30 μM (**Table 2**).

I_{Kur} Blockers

I_{Kur} channels are expressed specifically in the atrium and contribute to atrial repolarization by activating in an ultrarapid manner. I_{Kur} channels have attracted attention because the channel has been considered as a pharmacological target for atrial tachyarrhythmias such as atrial fibrillation (Courtemanche et al., 1999; Nattel et al., 2002). DPO-I, an I_{Kur} inhibitor, showed prolongation of action potentials in human atrial myocytes but not in ventricular myocytes (Lagrutta et al., 2006). In addition, a previous study reported that S9947, another I_{Kur} inhibitor, did not affect ventricular function and porcine ventricular myocytes, but it prolonged the atrial refractory period (Knobloch et al., 2002). In the present study, consistent with the previous reports, DPO-1, S9947, and 4AP (non-selective I_{Kur} inhibitor) showed prolongation in PWD30cF and PWD50cF, but not in CT (**Figure 4**). In addition, our results showed that the KCNA5 gene was more abundantly expressed in AMs than in CT (data not shown). These results suggest that the present system is feasible for detecting the effect of pharmacological compounds on the early repolarization phase through I_{Kur} channels.

Bradyarrhythmias

As for cardiac toxicity, in addition to QT prolongation related to lethal ventricular arrhythmias, life-threatening bradyarrhythmias are also critical rhythm disorders to be avoided. Gene expression patterns in AM suggested that the present system not only shows atrial characteristics but also nodal type cells. Our previous paper reported that retinoic acid-treated hiPS-CMs demonstrated nodal type properties as well as atrial type properties in the gene expression of SHOX2 and HCN4 (Nakanishi et al., 2019). Thus, AM would be useful to detect unexpected electrophysiological action of pharmacological compounds. In the present study, AM demonstrated not only atrial properties but also nodal type, as demonstrated by the increase observed in SHOX2 gene expression and spontaneous beating rates. In this regard, the present system would be useful to detect drug toxicity to induce critical rhythm disorders such as sick sinus syndrome.

I_{KAch} Agonists

I_{KAch} channels are expressed specifically in the atrium as well as I_{Kur}, and contribute to atrial repolarization and resting membrane potentials. The activation of the channel causes shortening and increased dispersion of refractory periods, and these induce atrial reentry following the onset of atrial fibrillation (Liu et al., 1997). In the present study, carbachol, an I_{KAch} agonist, showed a decrease in beating rate and rising slope in AM but not in CT. In the present study, we analyzed the data at the time point (10 min after addition of the drug); however, carbachol caused irregular beats early after application only in AMs (data not shown). This phenomenon suggests that carbachol-induced activation of I_{KAch} led to the increased dispersion of the refractory period, and thus, the optimal analysis time remains to be re-evaluated. In the present system, it is now feasible to evaluate the propensity for drug-induced tachyarrhythmias by comparing the chamber-specific effect of cardiac ion channels of pharmacological compounds.

Ca^{2+} Channel Blockers and Agonist

In the present study, we tested Ca^{2+} channel blockers (verapamil and diltiazem) and an agonist (Bay K 8644). As a result, both verapamil and diltiazem decreased membrane potential duration through the shortening of the plateau phase. On the other hand, Bay K 8644 prolonged membrane potentials, especially PWD30cF in AM as well as in CT. These responses are different from those seen in I_{Kur} blockers, which showed prolongation in AM, but not in CT. In addition, more strikingly, both verapamil and diltiazem caused arrest of spontaneous beating in all the tested samples in the AM at the maximal concentration (**Table 2**). The results may be ascribed to the involvement of nodal type cell type in AMs in which the Ca current plays an important role in generating pacemaker potentials.

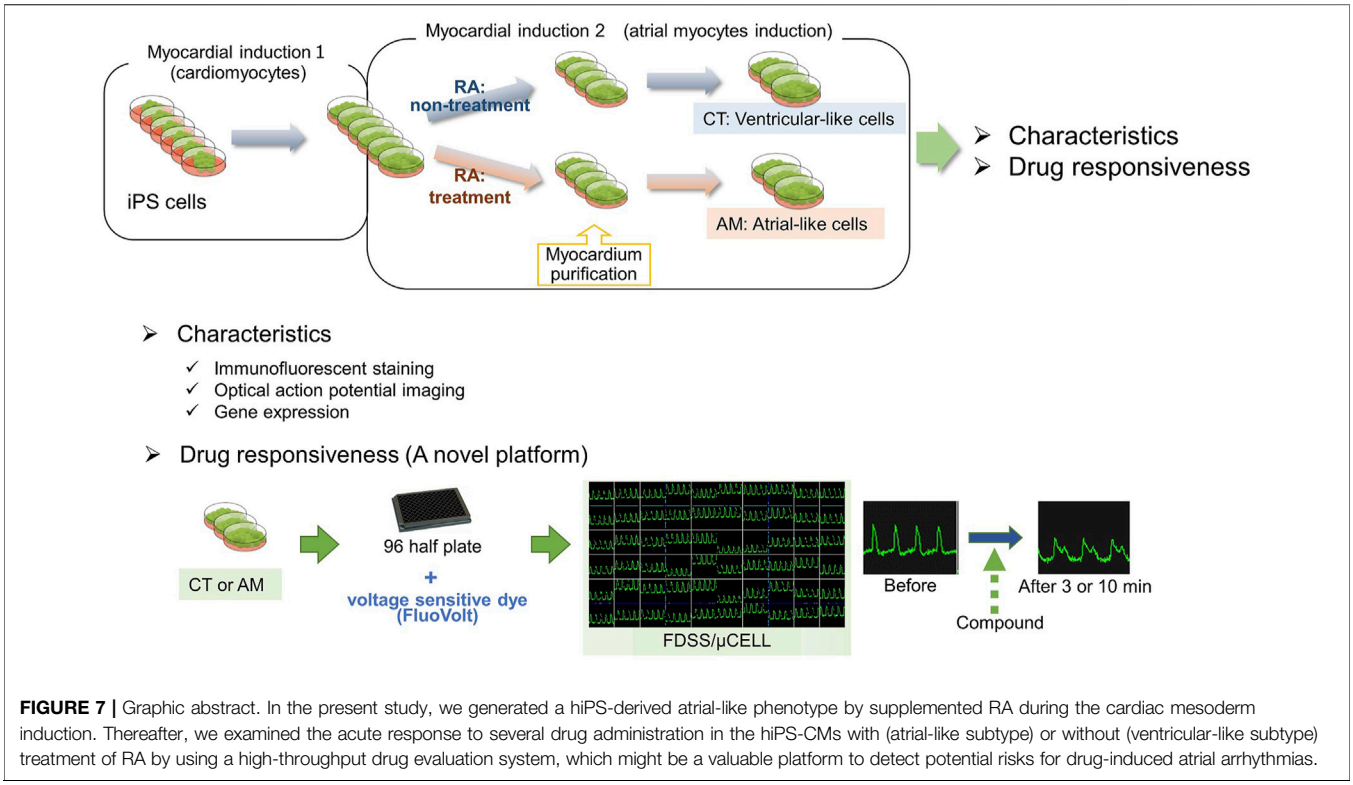

FIGURE 7 | Graphic abstract. In the present study, we generated a hiPS-derived atrial-like phenotype by supplemented RA during the cardiac mesoderm induction. Thereafter, we examined the acute response to several drug administration in the hiPS-CMs with (atrial-like subtype) or without (ventricular-like subtype) treatment of RA by using a high-throughput drug evaluation system, which might be a valuable platform to detect potential risks for drug-induced atrial arrhythmias.

Carbamazepine (Anti-epileptic Drug)

Carbamazepine is an antiepileptic drug that blocks neural Na channels, but the drug is also known to block the cardiac Na^+ channel (Nav1.5) with an IC_{50} of 152.0 μM (Harmer et al., 2011). In the present study, the drug showed a decrease in the rising slope and amplitude of membrane potentials in CT (**Figure 6**, **supplementary Figure 4**). In addition, carbamazepine caused the arrest of spontaneous beating when administered at a dose over 30 μM, more frequently in AM than in CT (**Table 2**). Carbamazepine has been reported to cause a decrease in Vmax and shortening of APD_{50} and APD_{90} in ventricular myocytes of guinea pigs at a concentration of 75 μM (Delaunois et al., 2015). Consistent with the previous study, the effects of carbamazepine on membrane potentials may be attributed to the inhibition of depolarization of ventricular myocytes through blocking of the Nav1.5 current. On the other hand, the membrane potentials of AM showed a decrease in the rising slope only at the maximal concentration. The results may be ascribed to the fact that Ca^{2+} channels, but not Na^+ channels, contribute to membrane potentials mainly in nodal cells, and thus AM were less sensitive to CBZ. The inhibition of the Na^+ current in both atrial-and node-type cells might cause the arrest of spontaneous beating at the maximal concentration.

Phenytoin (Anti-epileptic Drug)

Phenytoin is an antiepileptic drug with neural Na^+ channel blocking action, similar to the action exhibited by carbamazepine. In the present study, phenytoin showed an increase in the falling slope, a slight shortening of membrane potential duration, and arrest of spontaneous beating at concentrations higher than 30 μM in CT, while the drug caused arrests at concentrations higher than 10 μM in AM (**Figure 6**, **supplementary Figure 4**, **Table 2**). These results obtained with phenytoin were similar to those obtained with verapamil and diltiazem. Previous studies reported that phenytoin exhibits an inhibitory action on the cardiac Nav1.5 current and the Cav1.2 current with IC_{50} values of 72.4/120.6 μM and 21.9 μM, respectively Kramer et al., (2013), Harmer et al., (2011), demonstrating that the drug has stronger action on Cav1.2 than Nav1.5. Based on these data, it is conceivable that the results observed with the use of phenytoin in AM may be caused by its heterogenic cellular population including nodal type cells as well as atrial cells.

In the present study, various drugs demonstrated the arrest of spontaneous beatings in AM before the onset of the dysrhythmias in CT, and these results can be explained based on their actions on cardiac ion channels. These results strongly suggest that the detection of drug-induced bradyarrhythmias can be one of the important parameters in addition to the induction of tachyarrhythmias and the velocity/pattern of conduction.

CONCLUSION

We successfully established a platform for human iPS-derived cardiomyocytes with atrial and nodal properties by treatment with retinoic acid (**Figure 7**). Membrane potential-based drug testing on the present platforms would be useful to detect propensities for drug-induced tachyarrhythmias by comparing

ventricular and atrial drug responses. In addition, atrial platforms are more sensitive to bradyarrhythmias. This may be achieved with additional parameters for cardiac conduction.

These results suggest that the present evaluation system is useful for developing anti-atrial-arrhythmic drugs as well as for detecting potential risk for drug-induced atrial arrhythmias or rhythm/conduction disturbances.

MATERIALS AND METHODS

The study protocol was approved the Institutional Review Board of Osaka University and all experiments were performed under the guidelines of the Osaka University Gene Modification Experiments Safety Committee.

Cardiac Differentiation of hiPSC-CMs

hiPSCs from a healthy human (RIKEN BRC Cell Bank, Tsukuba, Japan) were subjected to cardiac differentiation using the PSC Cardiomyocyte Differentiation Kit (ThermoFisher SCIENTIFIC). Briefly, undifferentiated hiPSCs were maintained on iMatrix-511 (Nippi, 892,021) in StemFit® AK02N medium (Ajinomoto, AK02N) and passaged enzymatically at 80%–90% confluence.

The hiPSCs were enzymatically dispersed and maintained until 80% confluence with StemFit® AK02N containing 10 μM Y-27632 (Wako, 036-24023). The next day, the culture medium was changed to StemFit® AK02N without Y-27632, which was maintained until the next passage. hiPSCs were seeded on a dish coated with Geltrex LDEV-Free Reduced Growth Factor (ThermoFisher SCIENTIFIC) at 1% concentration in PBS. When the seeded cells reached 80% confluency (day-1), the culture medium was changed to StemFit® AK02N containing Matrigel® (Growth Factor Reduced, Corning, 354,230) at 1% concentration for 24 h. On day0, the culture medium was changed to Medium A (PSC Cardiomyocyte Differentiation Kit, ThermoFisher SCIENTIFIC) containing Matrigel for 48 h. On day2, the culture medium was changed to Medium B (PSC Cardiomyocyte Differentiation Kit, ThermoFisher SCIENTIFIC) for 48 h. On day4, the culture medium was changed to cardiomyocyte maintenance medium (PSC Cardiomyocyte Differentiation Kit, ThermoFisher SCIENTIFIC) supplemented with or without 0.7 μM RA (Sigma Aldrich, R2625) for 72 h. On day 7, the culture medium was changed to cardiomyocyte maintenance medium, and change the medium every 2 days. The cells typically started spontaneous beating around 10 days of initiation of the differentiation protocol. Purification of cardiomyocytes was performed by using a non-glucose medium supplemented with 4 mM lactic acid for 4days/time, performed 2 times (from day 14 to day 18, and from day 21 to day 25), between the 2 times of purifying application, the medium was changed to cardiomyocyte maintenance medium for 72 h (from day 18 to day 21). After purification, the culture was continued in the cardiomyocyte maintenance medium until the functional analysis.

Immunofluorescent Staining

hiPSC-derived cardiomyocytes were fixed with 4% PFA and permeabilized with 0.1% Triton-X in PBS (-) for 15 min at 4°C. Then, the cells were blocked with 5% BSA in PBS (-) for 60 min at room temperature. Primary antibodies were reacted for 24 h at 4°C, and secondary antibodies were reacted for 1 h at room temperature. Nuclei were labeled with Hoechst 33342 (Dojindo, H342). Primary antibodies were anti-Troponin T (clone 13-11) (1: 200, Thermo Scientific, MA5-12960), anti-MLC2a (1:200, Synaptic Systems, 311 011), and anti-MLC2v (1:200, ProteinTech, 10906-1-AP). Secondary antibodies were Alexa Fluor 488, donkey anti-mouse IgG (HCL), Alexa Fluor 568, donkey anti-rabbit IgG (HCL), Alexa Fluor 647, donkey anti-mouse IgG (HCL). Fluorescence images were obtained using Operetta high content imaging system (PerkinElmer, Japan) and analyzed using Harmony analysis software (PerkinElmer, Japan).

Optical Action Potential Imaging

hiPSC-CMs were loaded with a voltage-sensitive dye (FluoVolt™ Membrane Potential Kit, F10488, ThermoFisher SCIENTIFIC) for 30 min at RT. The excitation and emission wavelengths were 522 and 535 nm, respectively. Then, 10 μM blebbistatin (Wako, 027-17043), an excitation-contraction uncoupler, was applied to avert motion artifacts. All experiments were performed at 37°C under aerial conditions. Optical action potential (OAP) imaging was acquired at a sampling rate of 5 or 10 ms per frame using the MiCAM02 imaging system (Brainvision, Tokyo, Japan) equipped with a high-speed CMOS camera, alongside field-of-view and spatial resolution, which were 5.76 × 4.8 mm and 30 × 30 μm, respectively. OAP parameters including average CL, d (−F)/dt_{max}, and APD, were calculated using OriginPro 8.6J software (LightStone, Tokyo, Japan).

High-Throughput Recording of Membrane Potential Signal Recording

FluoVolt™ Membrane Potential Kit (ThermoFisher SCIENTIFIC, F10488, Massachusetts, United States) was used to measure membrane potentials. The basic procedure was performed in accordance with the manufacturer's instructions. Briefly, the loading dye solution was adjusted with an experimental medium (1% GlutaMAX supplement (ThermoFisher SCIENTIFIC), 1% HEPES (Sigma-Aldrich, Missouri, United States), and 0.001% Pluronic F-127 (Thermo Fisher Scientific) in FluoroBrite DMEM™ (ThermoFisher SCIENTIFIC). After washing the cells twice with the experimental medium, the loading dye solution was added and loaded for 30 min at 37°C. Thereafter, the cells were washed twice with the measurement buffer (1% GlutaMAX supplement, 1% HEPES, 2% fetal bovine serum in FluoroBrite DMEM™). Fluorescence signals representing the membrane potential were measured using FDSS/μCell imaging platform (Hamamatsu Photonics K.K., Hamamatsu, Japan). MP were recorded at excitation and emission stages at wavelengths of 470 and 540 nm, respectively. Measurements were taken during the pre-test, and 10min (except for Bay K 8644, the drug response time was 3 min) post-compound addition. Stock solutions of the test compounds were prepared in 100% DMSO, and serially diluted 1/40 into compound plates for testing (0.5% DMSO was the maximum concentration in all wells). The compounds were automatically pipetted from the compound plate, and 12 μL was loaded in the wells already containing the cells with 48 μL of media.

Recording data were analyzed using Waveform Analysis of Cardiomyocyte Software (Ver.1.2.1J, Hamamatsu Photonics K.K.). Data values for a well were averaged from waveforms that arose during 30 s. The beat rate (BR; beats per minute), waveform amplitude (AMP), and duration at 30, 50, and 80% of decay (PWD30, PWD 50, and PWD 80, respectively) were used as evaluation parameters. PWDs were corrected using the Fridericia formula. PWD30-80 was calculated as the difference between PWD80 and PWD30. Each parameter was calculated as percentage change (%) from the value before test compound addition.

Data Analysis

All data are expressed as mean ± standard deviation (SD). The data were confirmed as normal distribution by the Shapiro-Wilk test. Two independent groups were compared using the Student's t-test for homogeneity variance, and the heteroscedasticity variance by using Welch *t*-test. Multiple groups variance was compared using one-way analysis of variance (ANOVA), followed by Tukey's test. p values of <0.05 were considered statistically significant. Statistical analysis was performed using JMP Pro 14.0 (SAS, Tokyo).

DATA AVAILABILITY STATEMENT

The original contributions presented in the study are included in the article/**Supplementary Material**, further inquiries can be directed to the corresponding author.

ETHICS STATEMENT

The studies involving human participants were reviewed and approved by The Institutional Review Board of Osaka University. The patients/participants provided their written informed consent to participate in this study.

AUTHOR CONTRIBUTIONS

YH, ST, JL and J-KL conceptualized the study, designed and performed the experiments, analyzed the data, and wrote the manuscript. AH analyzed the data, reviewed the manuscript.

FUNDING

This study was supported in part by the Agency for Medical Research and Development, AMED (JP17bm0804008h0001 to J-KL), and Joint Research Grant (Sumitomo-Dainippon Pharma. CO., Ltd).

ACKNOWLEDGMENTS

The authors thank Hiroyuki Nakanishi for technical advice and discussion. The authors are grateful to Mayuko Matsushima, Hideki Yasutake, Yuki Kuramoto and Keiko Miwa for their technical advice and remarks. We would like to thank Editage (www.editage.jp) for language editing. The part of the present study first appeared in the conference paper of the 92nd Annual Scientific Meeting of the Japanese Pharmacological Society [YH. Nihon Yakurigaku Zasshi. 2020; 155(5):303-308]. The permission of the reuse of the contents was granted from the Japanese Pharmacological Society according to the Policies and Publication Ethics of Frontiers (https://www.frontiersin.org/about/policies-and-publication-ethics).

SUPPLEMENTARY MATERIAL

The Supplementary Material for this article can be found online at: https://www.frontiersin.org/articles/10.3389/fphar.2021.680618/full#supplementary-material

REFERENCES

Ando, H., Yoshinaga, T., Yamamoto, W., Asakura, K., Uda, T., Taniguchi, T., et al. (2017). A New Paradigm for Drug-Induced Torsadogenic Risk Assessment Using Human iPS Cell-Derived Cardiomyocytes. *J. Pharmacol. Toxicol. Methods* 84, 111–127. doi:10.1016/j.vascn.2016.12.003

Argenziano, M., Lambers, E., Hong, L., Sridhar, A., Zhang, M., Chalazan, B., et al. (2018). Electrophysiologic Characterization of Calcium Handling in Human Induced Pluripotent Stem Cell-Derived Atrial Cardiomyocytes. *Stem Cel Rep.* 10, 1867–1878. doi:10.1016/j.stemcr.2018.04.005

Berry, E. M., and Hasin, Y. (1978). Propranolol-Induced Dysfunction of the Sinus Node in Wolff-Parkinson-White Syndrome. *Chest* 73, 873–875. doi:10.1378/chest.73.6.873

Bordier, P., Garrigue, S., Barold, S. S., Bressolles, N., Lanusse, S., and Clementy, J. (2003). Significance of Syncope in Patients with Alzheimer's Disease Treated with Cholinesterase Inhibitors. *Europace*. 5 (4), 429-31. doi:10.1016/s1099-5129(03)00080-1

Chae, Y. J., Lee, H. J., Jeon, J. H., Kim, I.-B., Choi, J.-S., and Sung, K.-W. (2015). Effects of Donepezil on hERG Potassium Channels. *Brain Res.* 1597, 77-85. doi:10.1117/12.2081527

Chugh, S. S., Havmoeller, R., Narayanan, K., Singh, D., Rienstra, M., Benjamin, E. J., et al. (2014). Worldwide Epidemiology of Atrial Fibrillation. *Circulation* 129, 837–847. doi:10.1161/CIRCULATIONAHA.113.005119

Courtemanche, M., Ramirez, R. J., and Nattel, S. (1999). Ionic Targets for Drug Therapy and Atrial Fibrillation-Induced Electrical Remodeling: Insights from a Mathematical Model. *Cardiovasc. Res.* 42 (2), 477-489. doi:10.1016/S0008-6363(99)00034-6

Delaunois, A., Colomar, A., Depelchin, B. O., and Cornet, M. (2015). Cardiac Safety of Lacosamide: The Non-clinical Perspective. *Acta Neurol. Scand.* 132, 337–345. doi:10.1111/ane.12413

Devalla, H. D., Schwach, V., Ford, J. W., Milnes, J. T., El-Haou, S., Jackson, C., et al. (2015). Atrial-like Cardiomyocytes from Human Pluripotent Stem Cells Are a Robust Preclinical Model for Assessing Atrial-selective Pharmacology. *EMBO Mol. Med.* 7, 394–410. doi:10.15252/emmm.201404757

Edoute, Y., Nagachandran, P., Svirski, B., and Ben-Ami, H. (2000). Cardiovascular Adverse Drug Reaction Associated with Combined β-Adrenergic and Calcium Entry-Blocking Agents. *J. Cardiovasc. Pharmacol.* 35, 556–559. doi:10.1097/00005344-200004000-00007

Feric, N. T., and Radisic, M. (2016). Maturing Human Pluripotent Stem Cell-Derived Cardiomyocytes in Human Engineered Cardiac Tissues. *Adv. Drug Deliv. Rev.* 96, 110–134. doi:10.1016/j.addr.2015.04.019

Gassanov, N., Er, F., Zagidullin, N., Jankowski, M., Gutkowska, J., and Hoppe, U. C. (2008). Retinoid Acid-Induced Effects on Atrial and Pacemaker Cell Differentiation and Expression of Cardiac Ion Channels. *Differentiation* 76, 971–980. doi:10.1111/j.1432-0436.2008.00283.x

Harmer, A., Valentin, J.-P., and Pollard, C. (2011). On the Relationship between Block of the Cardiac Na+channel and Drug-Induced Prolongation of the QRS Complex. *Br. J. Pharmacol.* 164, 260–273. doi:10.1111/j.1476-5381.2011.01415.x

Hidaka, K., Lee, J. K., Kim, H. S., Ihm, C. H., Iio, A., Ogawa, M., et al. (2003). Chamber-specific Differentiation of Nkx2.5-positive Cardiac Precursor Cells from Murine Embryonic Stem Cells. *FASEB j.* 17, 740–742. doi:10.1096/fj.02-0104fje

Honda, Y. (2020). Availability of a Novel Cardiotoxicity Evaluation System Using Human Induced Pluripotent Stem Cell-Derived Atrial-like Myocytes. *Folia Pharmacol. Jpn.* 155, 303–308. doi:10.1254/fpj.20041

Jensen, M. O., Jogini, V., Borhani, D. W., Leffler, A. E., Dror, R. O., and Shaw, D. E. (2012). Mechanism of Voltage Gating in Potassium Channels. *Science* 336, 229–233. doi:10.1126/science.1216533

Jensen, P. N., Gronroos, N. N., Chen, L. Y., Folsom, A. R., Defilippi, C., Heckbert, S. R., et al. (2014). Incidence of and Risk Factors for Sick Sinus Syndrome in the General Population. *J. Am. Coll. Cardiol.* 64, 531–538. doi:10.1016/j.jacc.2014.03.056

Johnson, C. D., Rivera, H., and Jiménez, J. E. (1997). Carbamazepine-induced Sinus Node Dysfunction. *P. R. Health Sci. J.* 16 (1), 45-9.

Kho, J., Ioannou, A., Mandal, A. K. J., and Missouris, C. G. (2021). Donepezil Induces Ventricular Arrhythmias by Delayed Repolarisation. *Naunyn-schmiedeberg's Arch. Pharmacol.* 394, 559–560. doi:10.1007/s00210-020-02028-4

Knobloch, K., Brendel, J., Peukert, S., Rosenstein, B. x. r., Busch, A., and Wirth, K. (2002). Electrophysiological and Antiarrhythmic Effects of the Novel I Kur Channel Blockers, S9947 and S20951, on Left vs. Right Pig Atrium *In Vivo* in Comparison with the I Kr Blockers Dofetilide, Azimilide, D,l-Sotalol and Ibutilide. *Naunyn Schmiedebergs Arch Pharmacol.* 366, 482–487. doi:10.1007/s00210-002-0599-x

Kramer, J., Obejero-Paz, C. A., Myatt, G., Kuryshev, Y. A., Bruening-Wright, A., Verducci, J. S., et al. (2013). MICE models: Superior to the HERG model in predicting torsade de pointes. *Sci. Rep.* 3, 2100. doi:10.1038/srep02100

Kuwahata, S., Takenaka, T., Motoya, T., Masuda, K., Yonezawa, H., Shinchi, S., et al. (2021). Effect of QT Prolongation in Patients Taking Cholinesterase Inhibitors (Donepezil) for Alzheimer's Disease. *Circ. Rep.* 3, 115–121. doi:10.1253/circrep.CR-20-0115

Lagrutta, A., Wang, J., Fermini, B., and Salata, J. J. (2006). Novel, Potent Inhibitors of Human Kv1.5 K+ Channels and Ultrarapidly Activating Delayed Rectifier Potassium Current. *J. Pharmacol. Exp. Ther.* 317, 1054–1063. doi:10.1124/jpet.106.101162

Lane, D. A., Skjøth, F., Lip, G. Y. H., Larsen, T. B., and Kotecha, D. (2017). Temporal Trends in Incidence, Prevalence, and Mortality of Atrial Fibrillation in Primary Care. *Jaha* 6 (5), e005155. doi:10.1161/JAHA.116.005155

Lee, J. H., Protze, S. I., Laksman, Z., Backx, P. H., and Keller, G. M. (2017). Human Pluripotent Stem Cell-Derived Atrial and Ventricular Cardiomyocytes Develop from Distinct Mesoderm Populations. *Cell Stem Cell* 21, 179–194. doi:10.1016/j.stem.2017.07.003

Lemme, M., Ulmer, B. M., Lemoine, M. D., Zech, A. T. L., Flenner, F., Ravens, U., et al. (2018). Atrial-like Engineered Heart Tissue: An *In Vitro* Model of the Human Atrium. *Stem Cel Rep.* 11, 1378–1390. doi:10.1016/j.stemcr.2018.10.008

Liu, L., and Nattel, S. (1997). Differing Sympathetic and Vagal Effects on Atrial Fibrillation in Dogs: Role of Refractoriness Heterogeneity. *Am. J. Physiol.* 273, H805–H816. doi:10.1152/ajpheart.1997.273.2.H805

Ma, J., Guo, L., Fiene, S. J., Anson, B. D., Thomson, J. A., Kamp, T. J., et al. (2011). High Purity Human-Induced Pluripotent Stem Cell-Derived Cardiomyocytes: Electrophysiological Properties of Action Potentials and Ionic Currents. *Am. J. Physiology-Heart Circulatory Physiol.* 301, H2006–H2017. doi:10.1152/ajpheart.00694.2011

Moss, J. B., Xavier-Neto, J., Shapiro, M. D., Nayeem, S. M., Mccaffery, P., Dräger, U. C., et al. (1998). Dynamic Patterns of Retinoic Acid Synthesis and Response in the Developing Mammalian Heart. *Developmental Biol.* 199, 55–71. doi:10.1006/dbio.1998.8911

Nakanishi, H., Lee, J.-K., Miwa, K., Masuyama, K., Yasutake, H., Li, J., et al. (2019). Geometrical Patterning and Constituent Cell Heterogeneity Facilitate Electrical Conduction Disturbances in a Human Induced Pluripotent Stem Cell-Based Platform: An *In Vitro* Disease Model of Atrial Arrhythmias. *Front. Physiol.* 10, 818. doi:10.3389/fphys.2019.00818

Nakanishi, K., Sudo, T., and Morishima, N. (2005). Endoplasmic Reticulum Stress Signaling Transmitted by ATF6 Mediates Apoptosis during Muscle Development. *J. Cel Biol.* 169, 555–560. doi:10.1083/jcb.200412024

Nattel, S., Khairy, P., Roy, D., Thibault, B., Guerra, P., Talajic, M., et al. (2002). New Approaches to Atrial Fibrillation Management. *Drugs* 62, 2377–2397. doi:10.2165/00003495-200262160-00005

Nozaki, Y., Honda, Y., Watanabe, H., Saiki, S., Koyabu, K., Itoh, T., et al. (2017). CSAHi Study-2: Validation of Multi-Electrode Array Systems (MEA60/2100) for Prediction of Drug-Induced Proarrhythmia Using Human iPS Cell-Derived Cardiomyocytes: Assessment of Reference Compounds and Comparison with Non-clinical Studies and Clinical Information. *Regul. Toxicol. Pharmacol.* 88, 238–251. doi:10.1016/j.yrtph.2017.06.006

Rosenbloom, M. H., Finley, R., Scheinman, M. M., Feldman, M. D., Miller, B. L., and Rabinovici, G. D. (2010). Donepezil-associated Bradyarrhythmia in a Patient with Dementia with Lewy Bodies (DLB). *Alzheimer Dis. Assoc. Disord.* 24, 209–211. doi:10.1097/WAD.0b013e3181b7642b

Schnabel, R. B., Yin, X., Gona, P., Larson, M. G., Beiser, A. S., McManus, D. D., et al. (2015). 50 Year Trends in Atrial Fibrillation Prevalence, Incidence, Risk Factors, and Mortality in the Framingham Heart Study: A Cohort Study. *Lancet* 386 (9989), 154-62. doi:10.1016/S0140-6736(14)61774-8

Stockbridge, N., Morganroth, J., Shah, R. R., and Garnett, C. (2013). Dealing with Global Safety Issues. *Drug Saf.* 36, 167–182. doi:10.1007/s40264-013-0016-z

Thomsen, M. B., Matz, J., Volders, P. G. A., and Vos, M. A. (2006). Assessing the proarrhythmic potential of drugs: Current status of models and surrogate parameters of torsades de pointes arrhythmias. *Pharmacol. Ther.* 112, 150–170. doi:10.1016/j.pharmthera.2005.04.009

Watkins, P. B. (2011). Drug Safety Sciences and the Bottleneck in Drug Development. *Clin. Pharmacol. Ther.* 89, 788–790. doi:10.1038/clpt.2011.63

Xavier-Neto, J., Neville, C. M., Shapiro, M. D., Houghton, L., Wang, G. F., Nikovits, W., et al. (1999). A Retinoic Acid-Inducible Transgenic Marker of Sino-Atrial Development in the Mouse Heart. *Development* 126, 2677–2687. doi:10.1242/dev.126.12.2677

Zhang, Q., Jiang, J., Han, P., Yuan, Q., Zhang, J., Zhang, X., et al. (2011). Direct Differentiation of Atrial and Ventricular Myocytes from Human Embryonic Stem Cells by Alternating Retinoid Signals. *Cell Res* 21, 579–587. doi:10.1038/cr.2010.163

Conflict of Interest: Author YH was employed by the companies Sumitomo Dainippon Pharma Co. Ltd. and Sumika Chemical Analysis Service, Ltd. Author ST was employed by the company Sumitomo Dainippon Pharma Co. Ltd. J-KL and AH belonged to a joint research chair with the companies Sumitomo Dainippon Pharma Co. Ltd., Alpha MED Scientific, Inc. and SCREEN Holdings Co. Ltd.

The remaining authors declare that the research was conducted in the absence of any commercial or financial relationships that could be construed as a potential conflict of interest.

Publisher's Note: All claims expressed in this article are solely those of the authors and do not necessarily represent those of their affiliated organizations, or those of the publisher, the editors and the reviewers. Any product that may be evaluated in this article, or claim that may be made by its manufacturer, is not guaranteed or endorsed by the publisher.